ELSEVIER

Physica D 113 (1998) 134–151

PHYSICA D

Localized excitations in discrete nonlinear Schrödinger systems: Effects of nonlocal dispersive interactions and noise

K.Ø. Rasmussen [a], P.L. Christiansen [a,*], M. Johansson [a], Yu.B. Gaididei [b], S.F. Mingaleev [b]

[a] *Department of Mathematical Modelling, The Technical University of Denmark, DK-2800 Lyngby, Denmark*

[b] *Bogolyubov Institute for Theoretical Physics, 252 143 Kiev, Ukraine*

Abstract

A one-dimensional discrete nonlinear Schrödinger (DNLS) model with the power dependence, r^{-s} on the distance r, of dispersive interactions is proposed. The stationary states of the system are studied both analytically and numerically. Two kinds of trial functions, exp-like and sech-like are exploited and the results of both approaches are compared. Both on-site and inter-site stationary states are investigated. It is shown that for s sufficiently large all features of the model are qualitatively the same as in the DNLS model with nearest-neighbor interaction. For s less than some critical value, s_{cr}, there is an interval of bistability where two stable stationary states exist at each excitation number. The bistability of on-site solitons may occur for dipole–dipole dispersive interaction ($s = 3$), while s_{cr} for inter-site solitons is close to 2.1.

In the framework of the DNLS equation with nearest-neighbor coupling we discuss the stability of highly localized, "breather-like", excitations under the influence of thermal fluctuations. Numerical analysis shows that the lifetime of the breather is always finite and in a large parameter region inversely proportional to the noise variance for fixed damping and nonlinearity. We also find that the decay rate of the breather decreases with increasing nonlinearity and with increasing damping.

Keywords: Nonlocal dispersion; Long-range interaction; Competing length scales; Bistability; Nonlinear damping; Breathers; Noise

1. Introduction

This paper describes research on the localized solutions of the discrete nonlinear Schrödinger (DNLS) equation. Two quite different topics of this field will be addressed: Sections 2–4 are devoted to the investigation of nonlocal dispersive effects, while Section 5 describes the effect of noise.

Determination of the dynamical properties of physical systems with competition between discreteness, nonlinearity and dispersion has recently attracted a growing interest due to the wide applicability of such systems in various physical problems. Examples are coupled optical fibers, arrays of coupled Josephson junctions, nonlinear charge and excitation transport in biological macromolecules, elastic energy transfer in anharmonic chains, and charge transport in hydrogen-bonded systems. As is well known, the balance between nonlinearity and dispersion

* Correspoding author.

0167-2789/98/$19.00
PII S0167-2789(97)00261-3

in a weak nonlinearity (large dispersion) limit provides the existence of low-energy soliton-like excitations. Due to their robust character the solitonic excitations are important in the coherent excitation transport in biological macromolecules [1,2] and charge transport in organic semiconductors [3].

As a result of the interplay between discreteness, dispersion and nonlinear interactions intrinsically localized oscillatory states may appear and properties of the localized modes have been intensively studied during the past years [4,5]. For monoatomic lattices with a nearest-neighbor harmonic and quartic anharmonic interaction the localized states were found [5] to have nonlinear frequencies lying above the phonon band. In the case of one-dimensional nonlinear Schrödinger (NLS) lattice [6], a localized mode lying below the linear excitation band in the small amplitude limit reduces to the one-soliton solution of the continuum NLS equation.

In the main body of the previous research the dispersive interaction was assumed to be short ranged and therefore a nearest-neighbor approximation was used. However, there exist physical situations that definitely cannot be described appropriately in the framework of this approximation. Excitation transfer in molecular crystals [7] and vibron energy transport in biopolymers [2] are due to transition dipole–dipole interaction with $1/r^3$ dependence on the distance, r. The DNA molecule contains charged groups, with long-range Coulomb interaction $(1/r)$ between them. In systems where the dispersion curves of two elementary excitations are close or intersect, effective long-range transfer occurs. Such a situation arises for excitons and photons in semiconductors and molecular crystals (so-called polariton effects [7]).

Nonlinear waves in a one-dimensional chain with Lennard-Jones $(2n, n)$ interatomic potential were studied by Ishimori [8] who showed that the dynamics is governed by the Benjamin–Ono equation in the case $n = 2$ or by the Korteweg–de Vries equation for $n \geq 4$. Solitons in implicit form were obtained [9] in a sine-Gordon system with long-range interaction (LRI) of the Kac–Baker type [10] and the dependence of the soliton width and energy on the radius of the LRI was analyzed. A sine-Gordon equation with a nonlocal character of the nonlinear term was postulated in [11] and novel soliton states, of topological charge zero, were found to exist at large interaction radius. The effects of long-range harmonic interaction in a chain with short-range anharmonicity was considered in [12], and it was demonstrated that the existence of two velocity dependent competing length scales leads to two types of solitons with characteristically different width and shapes for two velocity regions separated by a gap. Effects of LRI of the Kac–Baker type were studied in static and dynamic nonlinear Klein–Gordon models [13]. Finally, a nonlocal NLS equation was proposed [14] to model systems with long-range dispersion effects. In contrast to the usual NLS equation stationary solutions only exist for a finite interval of the excitation number. In the upper part of this interval two different kinds of stationary solutions were found. The new kind which includes a cusp soliton was shown to be unstable. It was also pointed out that moving solitons radiate with a wavelength proportional to the velocity.

This paper exposes investigation of two types of soliton states in the discrete NLS model: on-site and inter-site states, and studies the motion of solitons and Peierls–Nabarro pinning. In Section 2 we present the analytical theory and the results of numerical simulations of stationary states of the discrete NLS model with a long-range dispersive interaction. We discuss the bistability phenomenon for the two types (on-site and inter-site) of soliton solutions. The analytical part of this section is based on a variational approach exploiting an exp-like function as a trial function. Then, in Section 3, we investigate the same problem with a sech-like trial function and compare the results of the two approaches. Section 4 is devoted to the investigation of the soliton motion in the discrete NLS model with a nonlocal dispersion. Equations describing the soliton center of mass motion are obtained and the properties coupled with a long-range character of the dispersion are discussed.

Finally, we describe in Section 5 the effects of noise on the localized excitations in the discrete NLS equation where only nearest-neighbor interaction is considered. The investigation is motivated by the need to understand the temperature effects in molecular systems, and a frequently used method to take into account effects of finite temperature in models describing a quantum quasiparticle (electron or exciton) interacting with lattice vibrations

is to add white noise and damping to the lattice equations [15], thereby turning these into Langevin equations. As was shown in [15], the coupled exciton–phonon equations can under certain approximations be reduced to a single DNLS equation describing the exciton dynamics, where the effects of thermal fluctuations of the phonons appear as a multiplicative noise term. The spectrum of the noise will then in general be colored, but assuming short correlation times it can be treated as white noise in a first approximation. In order to take proper account of the damping of the phonon system, it is necessary (at least when the white noise approximation is made) to additionally include a nonlinear damping term in the exciton equation [15]. With this inclusion, it was shown that energy balance may be established in the exciton system. On this background we consider in Section 5 the one-dimensional DNLS with multiplicative noise and nonlinear damping included, and investigate how these terms affect the discrete breathers.

2. Equations of motion

The model we study is described by the Hamiltonian

$$H = T + U = \frac{1}{2} \sum_{n,m(n\neq m)} J_{n-m} |\psi_m - \psi_n|^2 - \frac{1}{2} \sum_n |\psi_n|^4, \tag{1}$$

where T and U are the dispersive and the potential energy of the excitation, respectively. In Eq. (1) n and m are site indices and ψ_n is the excitation wave function. We investigate the model with the following power dependence on the distance of the matrix element of quasiparticle transfer $J_{n-m} = J/|n-m|^s$. The constant J characterizes the strength of the transfer and s is a parameter, being introduced to cover the different physical situations ranging from the nearest-neighbor approximation ($s = \infty$), dipole–dipole interaction ($s = 3$), to the long-range Coulomb interaction $s = 1$. In this paper, however, we shall restrict ourselves to $s > 1$. This "tunable" property of the equation illuminates both the competition between nonlinearity and dispersion and the interplay of LRI and lattice discreteness. From the Hamiltonian (1) we obtain the equation of motion $\mathrm{i}\dot{\psi}_n = \partial H/\partial \psi_n^*$ for the excitation wave function in the form

$$\mathrm{i}\dot{\psi}_n + \sum_{m(m\neq n)} J_{n-m}(\psi_m - \psi_n) + |\psi_n|^2 \psi_n = 0, \tag{2}$$

where the overdot denotes the time derivative. The Hamiltonian H and the number of excitations

$$N = \sum_n |\psi_n|^2 \tag{3}$$

are both conserved quantities. Stationary solutions of Eq. (2) in the form $\psi_n = \phi_n \exp(\mathrm{i}\Lambda t)$ with a nonlinear frequency Λ and a real valued profile ϕ_n are determined by

$$\Lambda\phi_n = J \sum_{m(m\neq n)} |n-m|^{-s}(\phi_m - \phi_n) + \phi_n^3. \tag{4}$$

Eq. (4) is the Euler–Lagrange equation for the problem of minimizing H under the constraint $N =$ constant. To obtain an approximate solution of the problem we use an ansatz for a localized state in the form

$$\phi_n = \sqrt{\frac{N \sinh\alpha}{\cosh(\alpha(2\delta - 1))}} \exp(-\alpha|n-\delta|), \tag{5}$$

where α is a trial parameter and δ is the position of the center of the localized state which without loss of generality can be restricted to $0 \leq \delta < 1$ for the infinite chain. The ansatz (5) is chosen to automatically satisfy the normalization

condition $\sum_n \phi_n^2 = N$. Performing some rather lengthy manipulations which are given in detail in [16] we can minimize the energy of the state (5) and thereby implicitly find the dependence N on Λ for the stationary state. Applying this result we shall study in detail the stationary states of the system, considering the following two types of stationary states: on-site ($\delta = 0$) and inter-site ($\delta = \frac{1}{2}$) separately. The numerical procedure used to solve the nonlinear eigenvalue problem (Eq. (4)) is similar to the method used in [17].

2.1. *On-site localized states:* $\delta = 0$.

Figs. 1 and 2 show the analytical as well as the direct numerical obtained dependence $N(\Lambda)$. A monotonic function is obtained for $s > s_{\rm cr}$, but for $s_{\rm cr} > s > 2$ the dependence becomes nonmonotonic (of $\mathcal{N}$-type) with a local maximum and a local minimum. These extrema coalesce at $s = s_{\rm cr} \simeq 2.72$ (from the analytical approach) and $s = s_{\rm cr} \simeq 3.03$ (from the numerical solution of Eq. (4)). For $s < 2$ the local maximum disappears. Thus the main features of all DNLS models with a power low dispersive interaction J_{n-m} decreasing faster than $|n-m|^{-s_{\rm cr}}$ coincide qualitatively with the features obtained in the nearest-neighbor approximation where only one on-site stationary state exists for any excitation number. However, in the case of the long-range nonlocal NLS equation (2) with $2 < s < s_{\rm cr}$ there exist for each N in the interval $[N_l(s), N_u(s)]$ three stationary states with nonlinear frequencies $\Lambda_1(N) < \Lambda_2(N) < \Lambda_3(N)$. In particular, this means that in the case of dipole–dipole interaction ($s = 3$) multiple solutions exist.

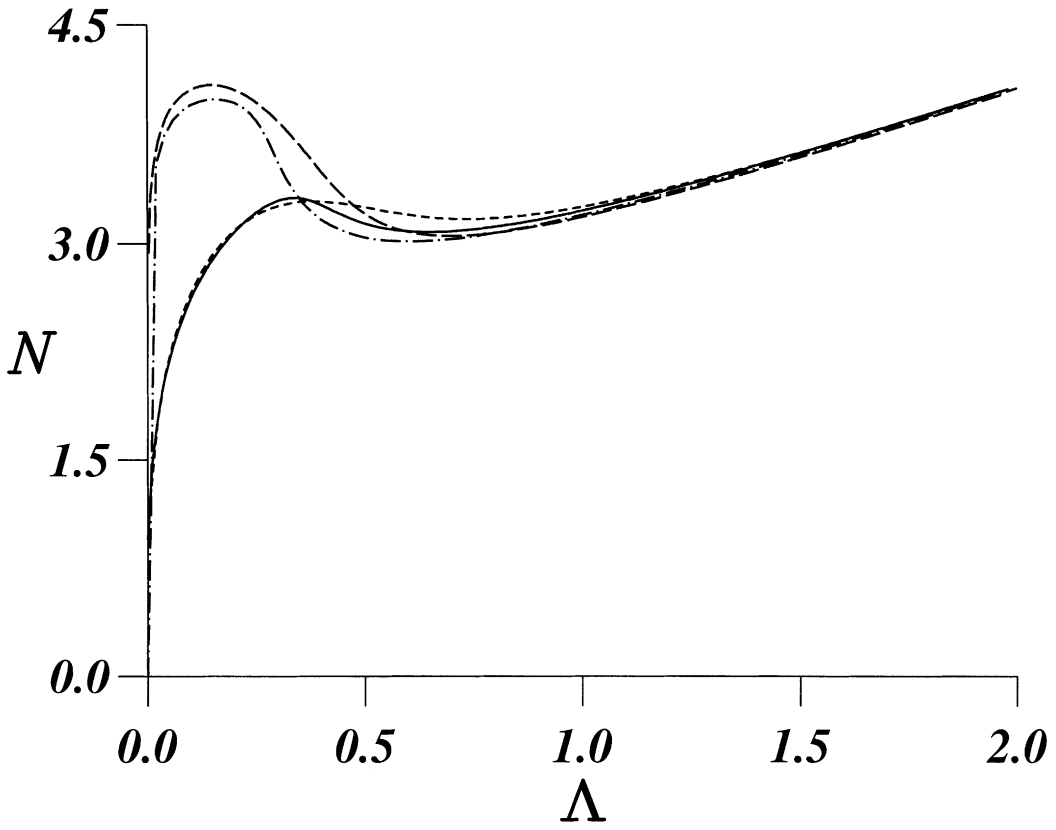

Fig. 1. Number of excitations, N, versus nonlinear frequency, Λ. Comparison between analytical dependence for $s = 2.1$ (long-dashed), 2.5 (short-dashed), and numerical dependence from Eq. (4) for $s = 2.1$ (dotted–dashed), and 2.5 (full).

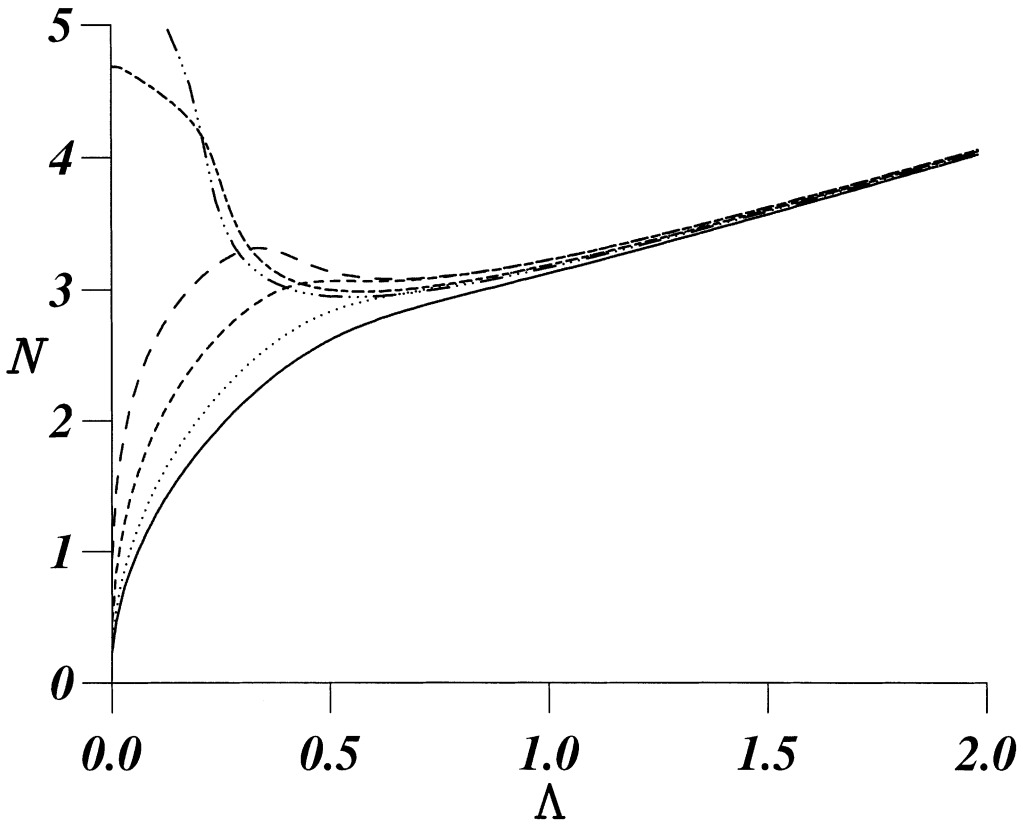

Fig. 2. Number of excitations, N, versus nonlinear frequency, Λ, numerically from Eq. (4) for $s = \infty$ (full), 4 (dotted), 3 (short-dashed), 2.5 (long-dashed), 2 (short–long-dashed), and 1.9 (dashed–dotted).

To investigate the stability properties of the different stationary states, we use the approach developed in [18] and find that the positive definiteness of the dispersion term T given by Eq. (1) and the form of the nonlinear term U permit generalization of the Laedke–Spatschek–Turitsyn theorem [18] to this nonlocal case. According to this theorem the necessary and sufficient stability criterion for on-site stationary states is

$$\frac{\mathrm{d}N}{\mathrm{d}\Lambda} = \frac{\mathrm{d}}{\mathrm{d}\Lambda} \sum_n \phi_n^2 > 0. \tag{6}$$

Therefore, we can conclude that in the interval $[N_\mathrm{l}(s), N_\mathrm{u}(s)]$ there are only two linearly stable stationary states ($\Lambda_1(N)$ and $\Lambda_3(N)$). The third state is unstable since $\mathrm{d}N/\mathrm{d}\Lambda < 0$ at $\Lambda = \Lambda_2$.

Fig. 3 shows that the three solutions differ significantly. The low frequency states are wide and continuum-like, while the high frequency solutions represent intrinsically localized states with a width of a few lattice spacings. For $s \gtrsim 2$ the inverse widths of the stable stationary states are, respectively,

$$\alpha_1 \approx \left(\frac{N}{8J}\right)^{1/(s-2)} = \left(\frac{N}{8J}\right)^{\ln l/(1-2\ln l)}, \qquad \alpha_3 \approx \ln\left(\frac{N}{J}\right), \tag{7}$$

where $l = \exp(1/s)$ is the characteristic range of the dispersive interaction which is defined as a distance at which the interaction decreases by a factor 2. It follows from these expressions that the existence of two so different soliton states for one value of the excitation number, N, is due to the presence of two different length scales in the system:

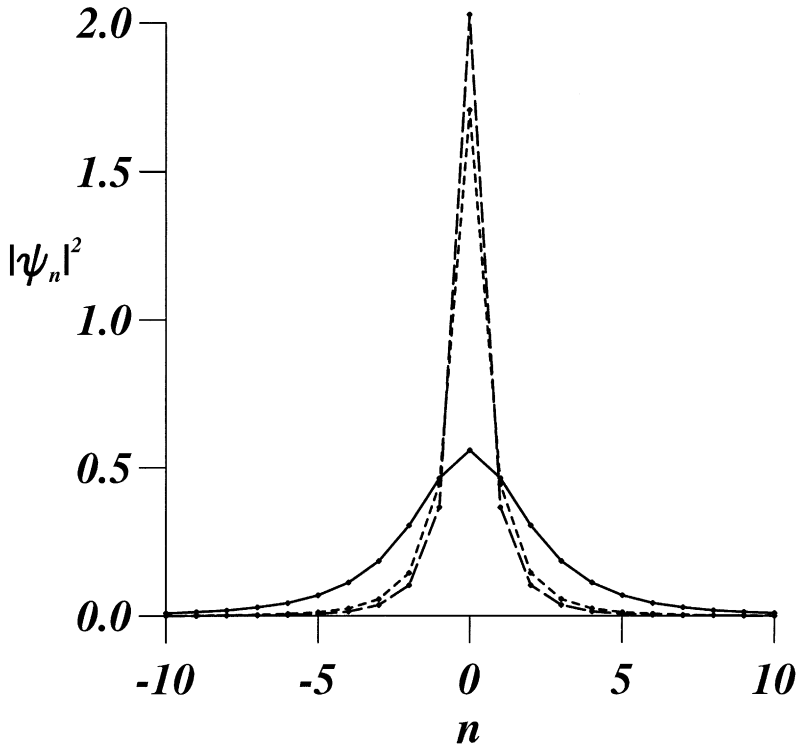

Fig. 3. Shapes of the three stationary states for $s = 2.5$ and $N = 3.1$. The stable: $\Lambda = 0.21$ (long-dashed), and $\Lambda = 0.74$ (full). The unstable: $\Lambda = 0.57$ (short-dashed).

the usual scale of the NLS model which is related to the competition between nonlinearity and dispersion (expressed in terms of the ratio N/J) and the range of the dispersive interaction l.

In the framework of the formalism developed in [16] the following approximate expressions can be obtained in the limit of large soliton width (small α)

$$N_{\mathrm{e}} = \frac{8\zeta(s-2)}{\zeta(s)}\alpha, \quad H_{\mathrm{e}} = -\frac{1}{8}N_{\mathrm{e}}^2\alpha \qquad \text{for } s > 3, \tag{8}$$

$$N_{\mathrm{e}} = \frac{8\pi(s-1)(s-2)}{\zeta(s)\Gamma(s)\sin(\pi s)}\alpha^{(s-2)}, \quad H_{\mathrm{e}} = -\frac{(s-2)}{4(s-1)}N_{\mathrm{e}}^2\alpha \qquad \text{for } s < 3, \tag{9}$$

$\zeta(s)$ denotes the Riemann zeta function and the subscript e on H and N signifies that an exponential trial function was used. The particular value $s = 2$ separates two different kinds of behavior: for $s > 2$, $N_{\mathrm{e}} \to 0$ while for $1 < s < 2$, $N_{\mathrm{e}} \to \infty$ as $\alpha \to 0$ and the stable continuum-like soliton disappears. This is confirmed by our simulation (see Fig. 2), which also indicates that the low frequency solitons in this case ($s < 2$) have algebraic tails, i.e., for $s = 1.9$, $\log\phi_n \simeq 6.3 - 2\log n$ when $n \gg 1$.

At the points ($\Lambda(N_{\mathrm{l}})$ and $\Lambda(N_{\mathrm{u}})$) the stability condition is violated, since $(\partial N/\partial\Lambda)_s$ vanishes. Constructing the locus of the end points we obtain the curve which is presented in Fig. 4. This curve bounds the region of bistability. It is analogous to the critical curve in the van der Waals' theory of liquid–vapour phase transition [19]. Thus in the present case we have a similar phase transition like behavior where the two phases are the continuum states and the intrinsically localized states, respectively. The analog of temperature is the parameter s.

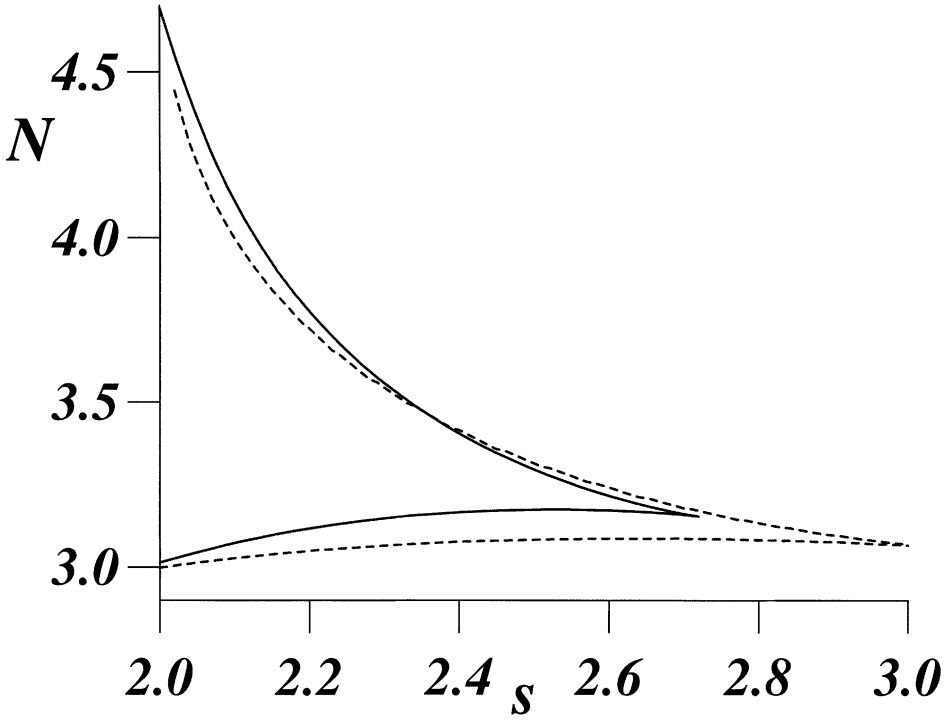

Fig. 4. End points of the bistability interval for N versus dispersion parameter s. For $s = s_{\mathrm{cr}}$ the end points coalesce. Analytical dependence (full), $s_{\mathrm{cr}} \simeq 2.72$. Numerical dependence (dashed), $s_{\mathrm{cr}} \simeq 3.03$.

2.2. *Inter-site localized states:* $\delta = \frac{1}{2}$

In Fig. 5 we plot the excitation number, N, as a function of nonlinear frequency Λ for inter-site localized states obtained from numerical solution of Eq. (4). The analytical results for $\delta = \frac{1}{2}$ are in qualitative agreement with numerical results but the quantitative agreement is not as good as in the on-site soliton case. The dependence displayed in Fig. 5 is similar to the dependence $N(\Lambda)$ obtained for on-site localized states (see Figs. 1 and 2) but with the following distinctions:

(i) While the $N(\Lambda)$-curves for on-site states tend to be independent of the dispersion parameters s at large Λ the similar curves for the inter-site states only become parallel as $\Lambda \to \infty$. The reason for this difference can be understood from the definition of the nonlinear frequency (see [16]) which yields

$$N = 2\Lambda + 4 - \frac{2}{\zeta(s)} \quad (\Lambda \to \infty), \quad \text{for } \delta = \tfrac{1}{2} \tag{10}$$

and

$$N = \Lambda + 2 \quad (\Lambda \to \infty) \quad \text{for } \delta = 0. \tag{11}$$

(ii) The critical value of the dispersion parameter $s'_{\mathrm{cr}} \simeq 2.1$ is much lower than the value obtained for on-site localized states.

(iii) The interval of s where the three inter-site states can exist, $2 < s < s'_{\mathrm{cr}}$, is very narrow. Thus, inter-site localized states are much less sensitive to the long-range character of the dispersion than the on-site states.

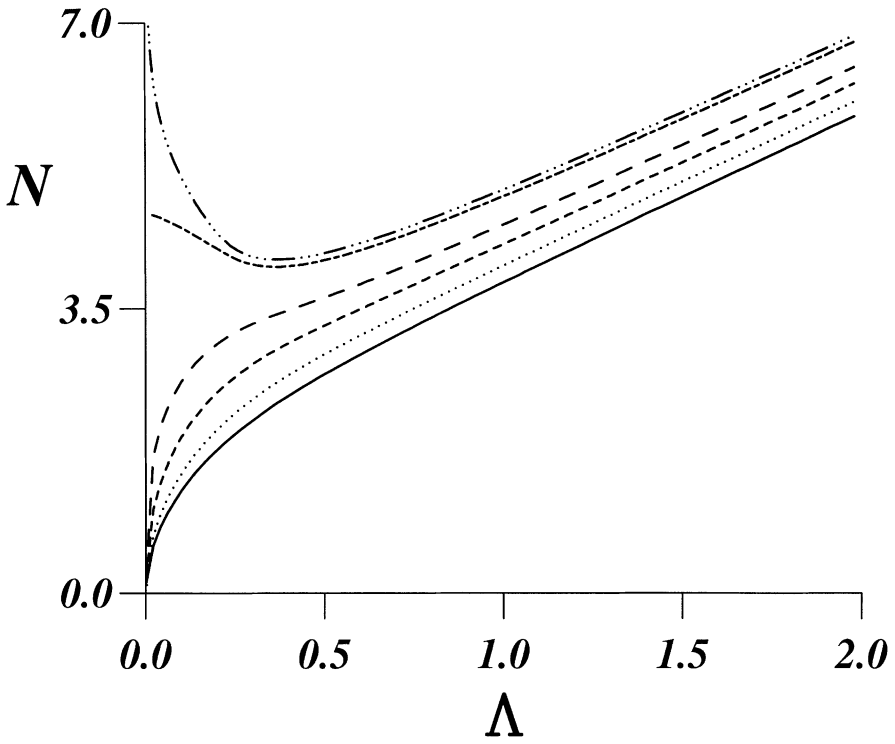

Fig. 5. Number of excitations, N, versus nonlinear frequency, Λ, numerically from Eq. (4) for $s = \infty$ (full), 4 (dotted), 3 (short-dashed), 2.5 (long-dashed), 2 (short–long-dashed), and 1.9 (dashed–dotted).

Three stationary inter-site states obtained for $s = 2.1$ and $N = 3.95$ are shown in Fig. 6. It is seen that similar to the case of on-site states the low frequency state is continuum-like while the high frequency solutions have a width of only a few lattice spacings.

For the parity-conserving (even) perturbations the stability condition of inter-site stationary states is the same as (6) but these excitations are unstable with respect to parity-nonconserving perturbations [18]. A typical evolution of these excitations is presented in Fig. 7. It is seen that choosing as an initial condition the inter-site state it transforms into an intrinsically localized on-site state with a time-dependent width.

3. Sech-like trial function approach

The ansatz

$$\phi_n = A\,\mathrm{sech}(\alpha(n-\delta)) \tag{12}$$

is known [20] to be a good representation of a localized state for small nonlinear frequencies Λ and small excitation numbers N in the discrete self-trapping model with nearest-neighbor excitation transfer ($s \to \infty$ in Eq. (4)). Therefore, the natural question arises whether the ansatz (12) is still good in the case of a long-range dispersive interaction. Clarifying this question we repeat the calculations from Section 2, using the trial function (12). Techniques developed in [21] permit us to obtain the kinetic energy of the excitations as

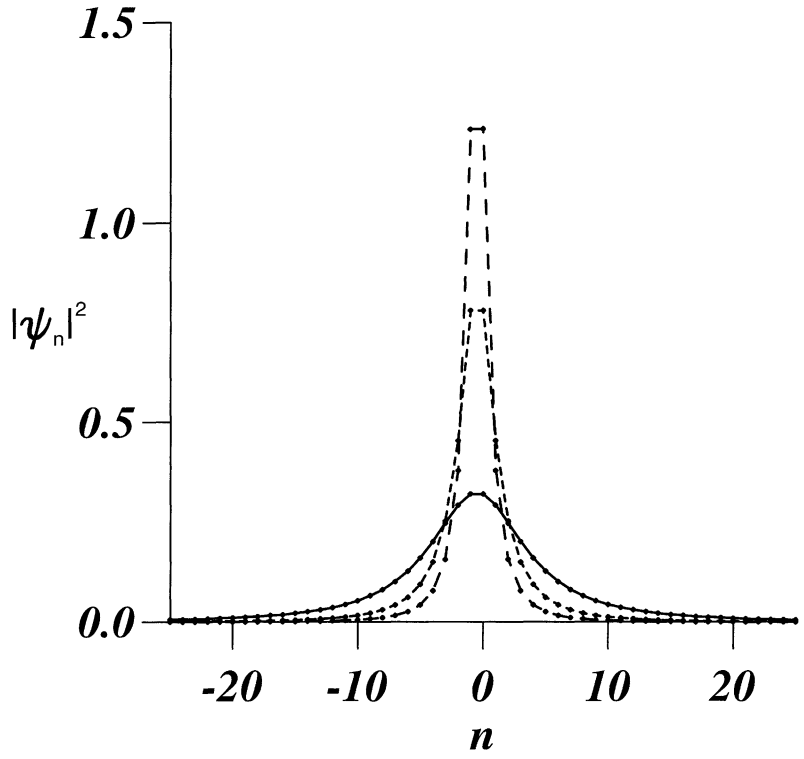

Fig. 6. Shapes of the three stationary states for $s = 2.1$ and $N = 3.95$. $\Lambda = 0.1$ (long-dashed), $\Lambda = 0.44$ (full), and $\Lambda = 0.24$ (short-dashed).

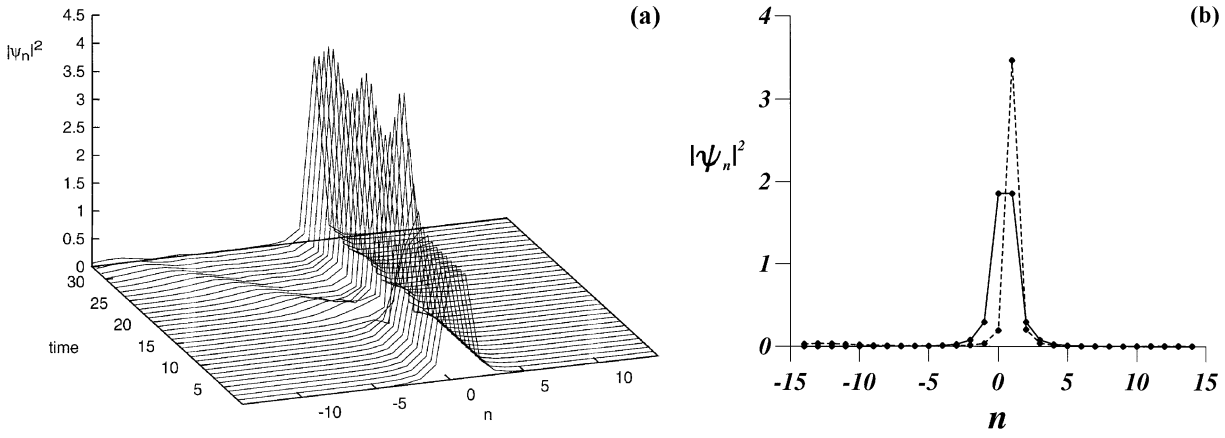

Fig. 7. (a) Evolution of an inter-site state $s = 2.57$, $N = 4.53$. (b) The inter-site state used as initial condition and the resulting on-site state at $t = 40$, where $N = 3.99$.

$$T(\delta) = 2JN - A^2 \sum_{n,m=-\infty}^{\infty} J_m \operatorname{sech}(\alpha(n-m-\delta))\operatorname{sech}(\alpha(n-\delta))$$
$$= 2JN - 4A^2 \frac{I(\alpha, s)}{\zeta(s)}, \tag{13}$$

with

$$I(\alpha, s) = \sum_{m=1}^{\infty} \frac{m^{1-s}}{\sinh(\alpha m)}$$
$$= \frac{\alpha^{s-2}\zeta(s-1)(1-2^{2-s})}{\pi^{s-2}\cos(\pi s/2)} + \sum_{r=0}^{\infty}(-1)^r \zeta(s-2r)\frac{(2^{2r}-2)}{(2r)!}|B_{2r}|\alpha^{2r-1}, \tag{14}$$

where B_{2r} are the Bernoulli numbers. In the same way the potential energy, U, of the localized state given by Eq. (12) is

$$U(\delta) = -\frac{1}{2}A^4 \sum_{n=-\infty}^{\infty} \operatorname{sech}^4(\alpha(n-\delta))$$
$$= -\frac{4A^4K'}{3\pi^2}\left\{ E' - \aleph^2 K' \operatorname{sn}^2(2\delta K) \right.$$
$$\left. + \frac{2}{\pi^2}\aleph^2 K'^3[\,1 - 2(1+\aleph^2)\operatorname{sn}^2(2\delta K) + 3\aleph^2 \operatorname{sn}^4(2\delta K)]\right\}. \tag{15}$$

Here the amplitude and the inverse width of the wave function are defined by the expression

$$A^2 = \frac{\pi^2 N}{4K'}(\,E' - \aleph^2 K' \operatorname{sn}^2(2\delta K)\,)^{-1}, \qquad \alpha = \pi\frac{K}{K'}. \tag{16}$$

In Eqs. (13)–(16) $K = K(\aleph)$ ($E = E(\aleph)$) is the complete elliptic integral of the first (second) kind, $\aleph$ is the modulus of the elliptic integrals, and $K' = K(\aleph')$, $E' = E(\aleph')$, where $\aleph' = (1-\aleph^2)^{1/2}$ is the modulus complementary to $\aleph$. $\operatorname{sn}(x)$ is a Jacobi elliptic function (for notation regarding elliptic functions and integrals see [22]).

For on-site localized states ($\delta = 0$) we obtain from the equation $\mathrm{d}(T+U)/\mathrm{d}\alpha = 0$ that the dependence of the excitation number, N, on the width of sech-like localized state is determined by Eq. (16) together with

$$N = 12\frac{(E'^2 - \aleph^2 K'^2)\, I(\alpha, s) + (\pi^2 E'/2K')\partial I(\alpha, s)/\partial\alpha)}{\aleph^2 K'^2 - E'^2 + (4K'^2/\pi^2)(\aleph^2 K' - E')(K' - E')}. \tag{17}$$

In the large soliton width (small α) limit we get from Eqs. (13)–(17) the energy and the excitation number of the system as

$$N_{\mathrm{s}} = \frac{4\zeta(s-2)}{\zeta(s)}\alpha, \quad H_{\mathrm{s}} = -\frac{1}{8}N_{\mathrm{s}}^2\alpha \qquad \text{for } s > 3, \tag{18}$$

and

$$N_{\mathrm{s}} = \frac{6(s-1)\zeta(s-1)(2^{2-s})}{\pi^{s-2}\zeta(s)\cos(\pi s/2)}\alpha^{s-2}, \quad H_{\mathrm{s}} = -\frac{1}{6}\frac{s-2}{s-1}2^{1/(2-s)}N_s^2\alpha \qquad \text{for } s < 3, \tag{19}$$

where the subscribed s on H and N signifies that a sech trial function was used. Comparing Eqs. (8) and (9) with Eqs. (18) and (19), respectively, we see that the continuum-like sech-like state is energetically more favorable than

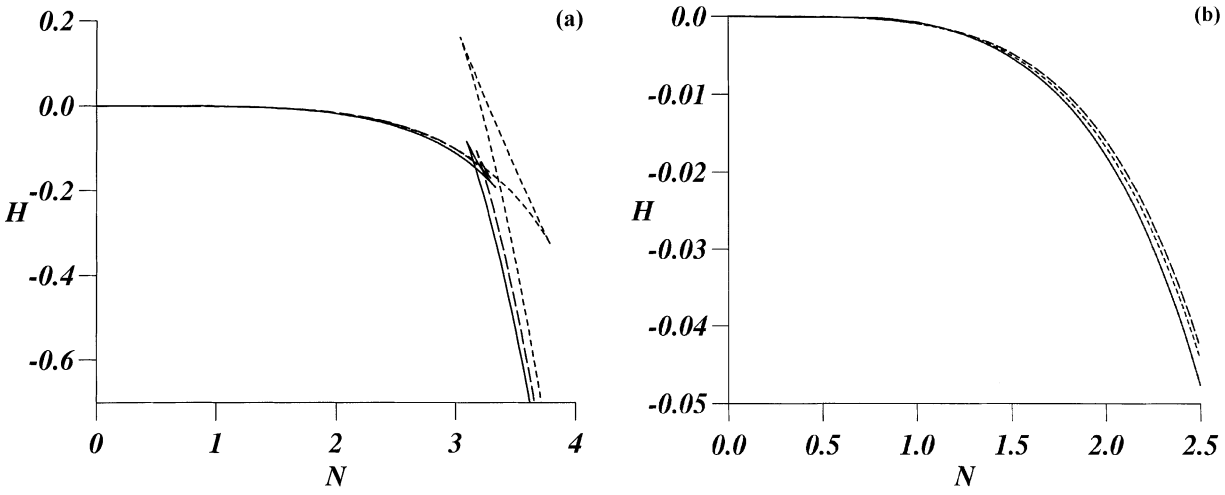

Fig. 8. The energy, H, versus N for the on-site stationary states at $s = 2.5$ in different scales is shown in (a) and (b). Numerical solution (full), exp-like trial function (long-dashed) and sech-like trial function (short-dashed).

the corresponding exp-like state for all values of the dispersion parameter s. Fig. 8 shows the energy H of the system as a function of excitation number, N, obtained analytically and numerically for $s = 2.5$. The existence of a bistability region manifests itself as a swallow tail structure in the dependence $H(N)$. It is seen that for excitation numbers, N, in the interval of bistability and for the values which correspond to the states of the second branch (intrinsically localized states $N > 3$), the H_e-curve agrees better than H_s-curve with the results of numerical simulations. This means that in this interval of the excitation number, N, the ground state is exp-like rather than sech-like.

4. Center of mass motion

In this section we shall discuss the motion of self-interacting excitations in the discrete chain with a long-range excitation transfer. In the nearest-neighbor approximation the problem was investigated in [23] using inverse-scattering transform techniques and an adiabatic approximation, and in [24] using a collective coordinate approach. We shall use the latter approach and postulate that the soliton wave function has the form

$$\psi_n(\beta, x) = A(x)\,\mathrm{sech}(\alpha\,(n - x(t))\mathrm{e}^{\mathrm{i}\beta(t)n}, \tag{20}$$

where $x(t)$ and $\beta(t)$ are the collective coordinates which approximately can be identified as the center of mass and the momentum of excitation, respectively. The width of the soliton (α^{-1}) is assumed to be time-independent and is determined by Eq. (17) while the amplitude $A(x)$ is given by Eq. (16). For $\alpha > 1$ the stationary state is so narrow that it is almost completely pinned by the lattice; therefore we limit our interest to the motion of the continuum-like excitations ($\alpha \leq 1$). As it was shown above the sech-like trial function is more appropriate than the exp-like trial function in this case. The Lagrangian of the system can be written as

$$L = \frac{\mathrm{i}}{2} \sum_n (\dot{\psi}_n\, \psi_n^* - \dot{\psi}_n{}^*\, \psi_n) - H, \tag{21}$$

where the Hamiltonian, H, is given by Eq. (1). Inserting Eq. (20) into Eq. (21) and using the following identity which holds for arbitrary x:

$$\frac{\mathrm{i}}{2}\sum_n (\dot{\psi}_n\,\psi_n^* - \dot{\psi}_n{}^*\psi_n) = -\dot{\beta}\left(x + A^2(x)\sum_{-\infty}^{+\infty}(n-x)\,\mathrm{sech}^2(\alpha\,(n-x))\right) = -\dot{\beta}(x + X(x)), \tag{22}$$

where

$$X(x) = -A(x)^2\frac{\partial}{\partial\alpha}\left(\frac{2K}{\alpha}\mathrm{zn}(2xK,\aleph)\right), \qquad \mathrm{zn}(u,\aleph) = \frac{\pi}{K}\sum_{n=1}^{\infty}\frac{\sin(\pi nu/K)}{\sinh(\pi nK'/K)}, \tag{23}$$

we obtain an effective Lagrangian of the system

$$L = -N(x + X(x))\,\dot{\beta} - T(\beta, x) - U(x), \tag{24}$$

where

$$\begin{aligned} T(\beta,x) &= 2NJ - \sum_{n,m} J_{n-m}\psi_n^*(\beta,x)\,\psi_m(\beta,x) \\ &= 2NJ - 4A^2(x)\frac{1}{\zeta(s)}\sum_{m=1}^{\infty}\frac{m^{1-s}\cos(\beta m)}{\sinh(\alpha m)}, \end{aligned} \tag{25}$$

and $U(x)$ is given by Eq. (15). In Eq. (23) zn denote the Jacobian zeta function. The Euler–Lagrange equations for β and x yield

$$N\left(1 + \frac{\mathrm{d}X}{\mathrm{d}x}\right)\dot{\beta} = -\frac{\partial}{\partial x}(T(\beta,x) + U(x)), \quad N\left(1 + \frac{\mathrm{d}X}{\mathrm{d}x}\right)\dot{x} = \frac{\partial}{\partial\beta}T(\beta,x). \tag{26}$$

For $\alpha \leq 1$ we can, expanding the functions $U(x)$ and $A^2(x)$ with respect to the small quantity $\exp(-\pi^2/\alpha)$, obtain from Eq. (26)

$$\dot{x} = \frac{2\alpha}{\zeta(s)}\sum_{m=1}^{\infty}\frac{m^{2-s}\,\sin(\beta m)}{\sinh(\alpha m)}, \qquad \dot{\beta} = -\frac{\partial}{\partial x}\mathcal{U}(x), \tag{27}$$

where

$$\mathcal{U}(x) = -\left(\frac{2\pi^4}{3\alpha^2}N - \frac{8\pi^2}{\zeta(s)}I(\alpha,s)\right)\mathrm{e}^{-\pi^2/\alpha}\cos(2\pi x). \tag{28}$$

The equations for the collective coordinates β and x in the form (27) and (28) were obtained using that: (i) the function $X(x)$, which characterizes the difference between the true center of mass of the soliton $\sum_n n|\psi_n|^2$ and the collective coordinate $x(t)$, is exponentially small and can be neglected within a chosen accuracy; and (ii) that the dependence $\mathrm{d}X/\mathrm{d}x$ in the l.h.s and the x dependence in the r.h.s of Eq. (26) can be omitted.

It is evident that the set of Eqs. (27) and (28) constitutes a Hamiltonian system, with the Hamiltonian

$$\mathcal{H} = \mathcal{T}(\beta) + \mathcal{U}(x), \tag{29}$$

where

$$\mathcal{T}(\beta) = -\frac{2\alpha}{\zeta(s)}\sum_{m=1}^{\infty}\frac{m^{1-s}\cos(\beta m)}{\sinh(m\alpha)}. \tag{30}$$

Hence the motion of the soliton can be viewed as a point particle described by the general coordinates β and x in an effective periodic Peierls–Nabarro potential $\mathcal{U}(x)$. The stationary point $x = 0$ and $\beta = 0$ is stable when the inverse

width, α, of the soliton is defined by Eqs. (18) and (19). In the nearest-neighbor approximation ($s \to \infty$) only the term with $m = 1$ survives in Eq. (30) and the kinetic energy becomes $\mathcal{T}(\beta) = -(2\alpha/\sinh(\alpha))\cos(\beta)$ in agreement with [23], [24]. For finite s and particularly for $s \leq 3$ the situation becomes more complicated. Indeed considering the case of small β we can expand the kinetic energy given by Eq. (30) and write

$$\mathcal{T} = \frac{\beta^2}{2M}. \tag{31}$$

Here the effective mass M has the form $M = \zeta(s)[2\alpha I(\alpha, s-2)]^{-1}$ and the function $I(\alpha, s)$ is defined by Eq. (14). It is seen from Eq. (14) that in contrast to the nearest-neighbor approximation where the mass M in the small velocity limit ($\beta \ll 1$) does not depend on the width of the soliton (on the excitation number, N), the long-range character of the excitation transfer for $s \leq 3$ facilitates the motion of solitons with large widths by decreasing the effective mass.

5. Noise effects

The form of the DNLS equation considered here is the following:

$$\mathrm{i}\dot{\psi}_n + J(\psi_{n+1} + \psi_{n-1}) + \gamma|\psi_n|^2\psi_n - \eta\psi_n\frac{\mathrm{d}}{\mathrm{d}t}(|\psi_n|^2) + h_n(t)\psi_n = 0, \tag{32}$$

where the last two terms describe nonlinear damping and multiplicative Gaussian white noise, respectively. The noise is assumed to have zero mean and variance $2D$, i.e.,

$$\langle h_n(t)\rangle = 0, \quad \langle h_n(t)h_n'(t')\rangle = 2D\delta(t-t')\delta_{nn'}. \tag{33}$$

Eq. (32) can be derived from the equation of motion for a quantum quasiparticle (e.g. electron or exciton) treated in the nearest-neighbor tight-binding approximation and interacting with a classically treated optical phonon field in contact with a heat bath, i.e. (in units of $\hbar = 1$)

$$\mathrm{i}\dot{\psi}_n + J(\psi_{n+1} + \psi_{n-1}) + \chi u_n\psi_n = 0, \tag{34}$$

$$M\ddot{u}_n + M\lambda\dot{u}_n + M\omega_0^2 u_n - \chi|\psi_n|^2 = \sigma_n(t). \tag{35}$$

Here ψ_n is the amplitude of the quasiparticle wave function at site n and u_n represents the elastic degree of freedom at site n. Furthermore, J is the nearest-neighbor hopping constant, χ the coupling constant between the quasiparticle and the phonons, M the molecular mass, λ a damping coefficient, ω_0 is the Einstein frequency of each oscillator, and $\sigma_n(t)$ is a stochastic force acting on the phonon system. Eq. (35) is the Langevin equation for the phonon-system, so the variance of the stochastic force is related to the external temperature T and the damping coefficient λ according to the fluctuation–dissipation theorem. The DNLS can be derived from Eqs. (34) and (35) if the quasiparticle field is assumed to vary slowly in time compared with the lattice vibrations [15]. This results in the following relation between the parameters of Eqs. (32)–(35):

$$\gamma = \frac{\chi^2}{M\omega_0^2}, \quad \eta = \gamma\frac{\lambda}{\omega_0^2}, \quad D = \eta k_\mathrm{B}T, \tag{36}$$

where k_B is the Boltzmann constant.

The DNLS equation has as its only conserved quantity the excitation number, Eq. (3), while the Hamiltonian d

$$H_\mathrm{DNLS} = -J\sum_n\left(\psi_n\psi_{n+1}^* + \psi_n^*\psi_{n+1}\right) - \frac{\gamma}{2}\sum_n|\psi_n|^4, \tag{37}$$

will evolve according to

$$\frac{\mathrm{d}H_{\mathrm{DNLS}}}{\mathrm{d}t} = -\eta \sum_n \left(\frac{\mathrm{d}}{\mathrm{d}t}(|\psi_n|^2) \right)^2 + \sum_n h_n(t) \frac{\mathrm{d}}{\mathrm{d}t} \left(|\psi_n|^2 \right) \tag{38}$$

indicating that the damping and noise terms in average provide dissipation and energy input, respectively.

We integrate Eq. (32) numerically using a single-site initial condition,

$$\psi_n(0) = \delta_{n,n_0}, \tag{39}$$

varying the parameters γ, η and D for the fixed values $N = 1$ and $J = 1$, and using a lattice large enough to simulate an infinite chain. For this choice of initial condition the DNLS exhibits a self-trapping transition at $\gamma = \gamma_c \simeq 3.5$ when $\eta = D = 0$; when $\gamma > \gamma_c$ a finite part of the excitation will remain trapped around the initial site during the time-evolution [25]. As γ is increased beyond γ_c, the total excitation number of the part trapped around the initial site increases, and the width of the excitation decreases. In the calculations reported here, we consider nonlinearities $\gamma \geq 5$, for which the trapped excitation has a highly discrete, breather-like nature.

An illustration of how the presence of noise in Eq. (32) affects the DNLS breathers is given in Figs. 9 and 10. We see that after a short initial interval, where the breather is created and the initial-site probability $|\psi_{n_0}|^2$ rapidly drops to a value close to its stationary value in the absence of noise, the noise will cause a slow, almost linear, decrease of the breather-intensity with time. This linear decay continues until the value of $|\psi_{n_0}|^2$ has been reduced to approximately half its initial value, at which point the initial-site probability rapidly drops to values close to zero, signifying that the breather is destroyed. After this point the system behaves diffusively, similar to the corresponding linear system ($\eta = \gamma = 0$), with the initial-site probability decaying in average as $t^{-1/2}$. Thus, we find that the lifetime of the breather is always finite, but increases when (a) the nonlinearity γ is increased, (b) the nonlinear damping η is increased, or (c) the noise variance D is decreased (see Fig. 10). The quantitative influence of the parameters γ, η and D on the lifetime has been investigated by performing numerical calculations for several different realizations of the noise, and determining the decay rate, κ, as the mean-value of $-\mathrm{d}(|\psi_{n_0}|^2)/\mathrm{d}t$ in the time-interval of almost linear decay. Some of these results are displayed in Fig. 11. Fig. 11(a) indicates that the decay rate is proportional to the variance of the noise over a large parameter region. We found this proportionality to be valid as long as the noise is so weak that the creation of the breather is unaffected (if the noise is too strong, no breather-like state will be created, and the diffusive spreading starts immediately). As is shown in Fig. 11(b), the

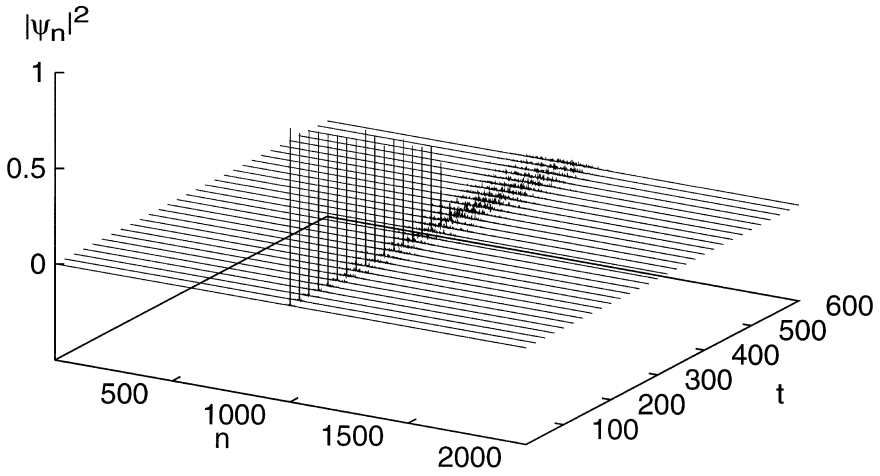

Fig. 9. Evolution of an initially single sited localized excitation. Parameter values are $\gamma = 10$, $\eta = 2$, and $D = 0.05$.

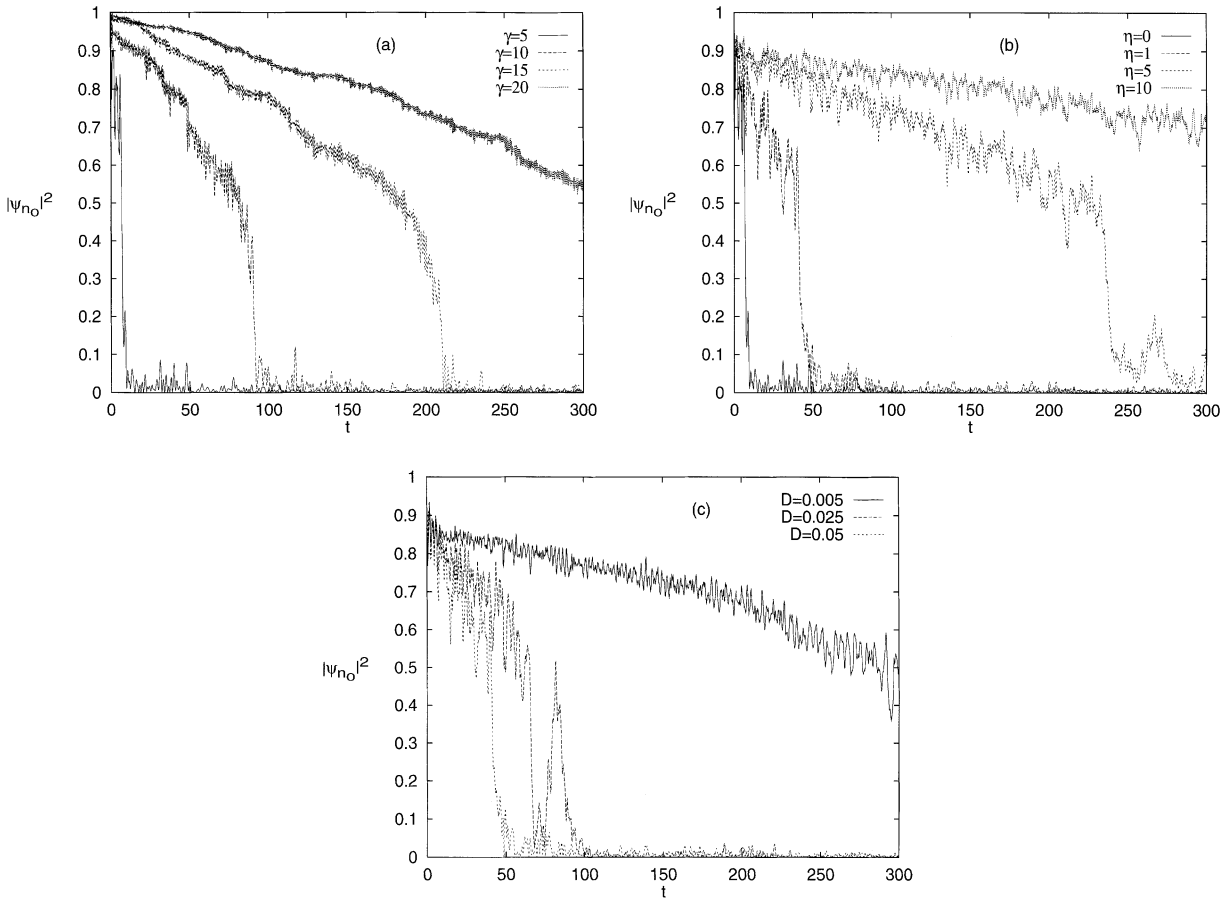

Fig. 10. Typical evolution of the initial-site probability for different values of γ, η, and D. In (a) we have $\eta = 0$, $D = 0.05$, and from bottom to top $\gamma = 5$, 10, 15, and 20; in (b) $\gamma = 5$, $D = 0.05$ and from bottom to top $\eta = 0$, 1, 5, and 10; in (c) $\gamma = 5$, $\eta = 1.0$, and $D = 0.005$, 0.025, and 0.05 from top to bottom. The particular realization of the noise is the same in all cases.

decay rate is for fixed D and η approximately proportional to γ^{-2} in the studied parameter range, while the data in Fig. 11(c) showing the variation of κ with η do not seem to follow any simple scaling law.

In order to gain some analytical understanding of the effects imposed on the DNLS breathers by the presence of noise and nonlinear damping, we use a method of collective coordinates similar to the approach used in Section 4. This approach necessitates a rather elaborated analysis where a Fokker–Planck equation describing the average dynamics of the system is derived. From this Fokker–Planck equation it is possible (all details can be found in [26]) to find the following approximative expression for the evolution of the probability at the initial site,

$$\langle |\psi_{n_0}|^2 \rangle \simeq 1 - \frac{2J^2}{\gamma^2} - \frac{6DJ^2}{\gamma^2} t \tag{40}$$

for $t \ll \gamma/6\eta J^2$. This result shows that the collective coordinate approach explains qualitatively the initial linear decay of the breather observed in the numerical simulations. The coefficient $6DJ^2/\gamma^2$ exhibits the same dependence of D/γ^2 as was observed numerically. Additionally we find that the prefactor $6J^2$ is of the same order of magnitude as what was found numerically. However, due to the approximate character of the analytical approach, the η-dependence predicted by Eq. (40) differs from the numerical results.

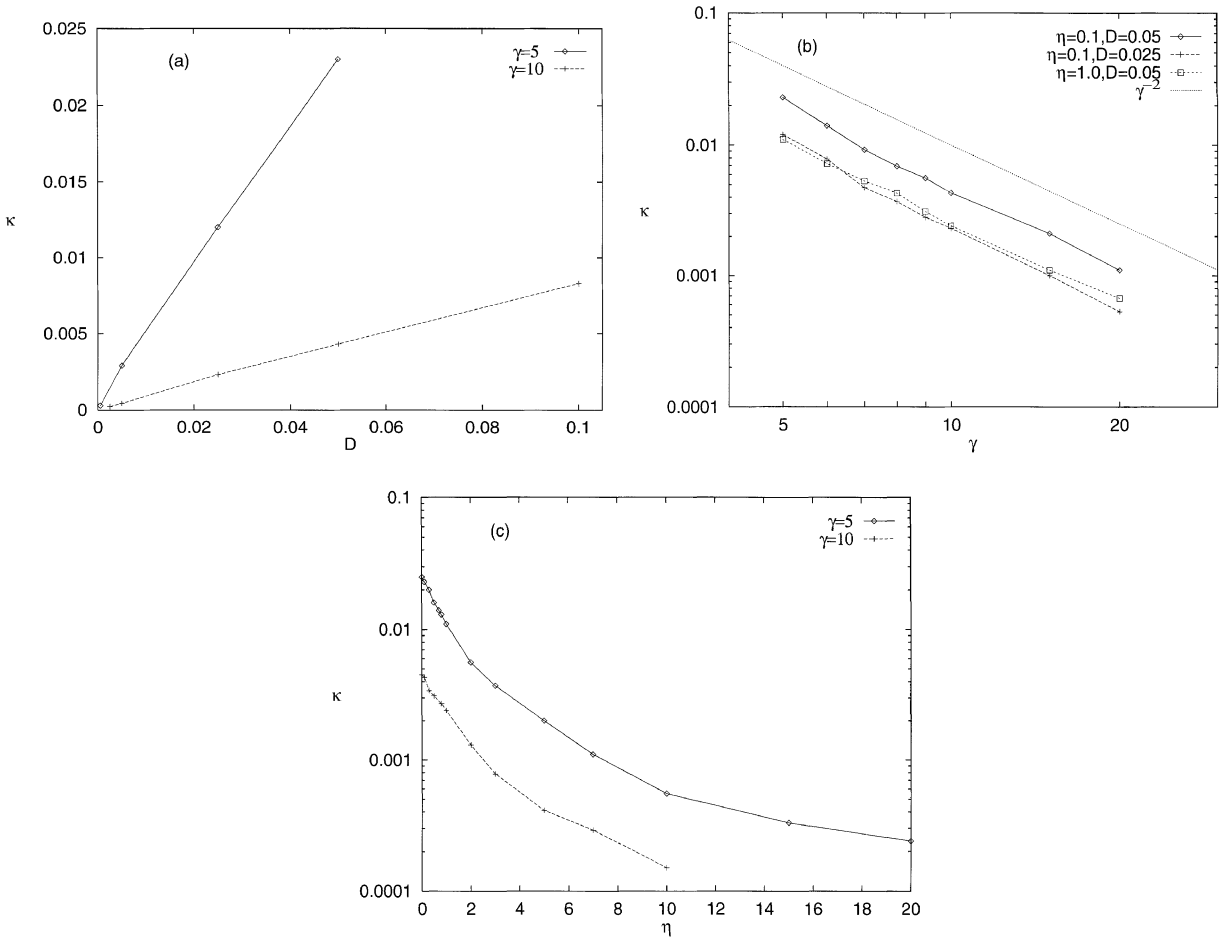

Fig. 11. Quantitative dependence of the decay rate, κ, of the breather as a function of (a) noise strength D, (b) nonlinearity parameter γ, and (c) nonlinear damping parameter η. In (a) $\eta = 0.1$ for both curves and in (c) $D = 0.05$ for both curves; other parameter values are as indicated in the figures.

6. Conclusion

In summary, a nonlocal discrete NLS equation has been proposed as a model for self-interacting excitations with power dependence r^{-s} on the distance r of the dispersive interactions. We have shown that the behavior of all NLS models with dispersion interaction decreasing faster than $r^{-s_{cr}}$ is qualitatively the same as the NLS model with a nearest-neighbor excitation transfer. In contrast to this there is an excitation number interval of bistability in the NLS models with a long-range dispersive interaction $s < s_{cr}$. In the interval $2 < s < s_{cr}$ two stable stationary states exist at each excitation number N. One of these states is a continuum-like soliton while the other one is an intrinsically localized mode. The existence of the bistability phenomenon in the NLS models with a nonlocal dispersion is a result of the competition of two length scales which exist in the system: the scale related to the competition between nonlinearity and dispersion, and the scale related to the dispersion interaction. Two types of stationary states have been considered: on-site and inter-site states. We found that the critical value of the dispersion parameter s_{cr} for the inter-site state is slightly above 2 while for the on-site stationary state it exceeds 3. This means that the bistable behavior may occur in the case of self-interacting excitations with the dipole–dipole excitation transfer.

We have shown that the motion of solitons in discrete NLS models with a long-range interaction can be viewed as the motion of a point particle in an effective periodic Peierls–Nabarro potential. In contrast to systems with nearest-neighbor interaction the mass of the particle depends on the excitation number and becomes smaller when the width of the soliton increases.

Finally, we have found that introducing multiplicative white noise and nonlinear damping into the discrete NLS equation with nearest-neighbor coupling will cause decay of the self-trapped discrete breathers which are created for large nonlinearities. A numerical analysis showed that the intensity at the central breather-site would initially decrease approximately linearly with time. The decay rate was found to decrease with increasing nonlinearity γ and with increasing damping η, and to increase with increasing noise variance D.

Acknowledgements

We thank J.J. Rasmussen, and V.K. Mezentsev for helpful discussions. One of the authors (YuBG) thanks the Department of Mathematical Modelling and MIDIT, The Technical University of Denmark, where part of this work was done under grant SNF 11-0921-1 from the Danish Natural Research Council and also acknowledges support from The Ukrainian Government and International Science Foundation under grant NK59100. MJ acknowledges the Swedish Foundation for International Cooperation in Research and Higher Education for financial support.

References

[1] A.S. Davydov, Soliton in Molecular Systems, Reidel, Dordrecht, 1985.
[2] A.C. Scott, Phys. Rep. 217 (1992) 1.
[3] W.P. Su, J.R. Schrieffer, A.J. Heeger, Phys. Rev. B 22 (1980) 2099; A.R. Bishop, D.K. Campbell, P.S. Lomdahl, B. Horovitz, S.R. Phillpot, Phys. Rev. Lett. 52 (1984) 671.
[4] M.J. Ablowitz, J.F. Ladik, Stud. Appl. Math. 55 (1976) 213; A.C. Scott, L. MacNeil, Phys. Lett. A 98 (1983) 87; D.N. Christodoulides, R.I. Joseph, Opt. Lett. 13 (1988) 794; A.J. Sievers, S. Takeno, Phys. Rev. Lett. 61 (1988) 970; J.C. Eilbeck, R. Flesh, Phys. Lett. A 149 (1990) 200; T. Dauxois, M. Peyrard, A.R. Bishop, Phys. Rev. E 47 (1993) 684; R.S. MacKay, S. Aubry, Nonlinearity 7 (1994) 1623.
[5] V.M. Burlakov, S.A. Kiselev, V.N. Pyrkov, Phys. Rev. 42 (1990) 4921; R. Bourbonnais, R. Maynard, Phys. Rev. Lett. 64 (1990) 1397; S.R. Bickham, A.J. Sievers, Phys. Rev. B 43 (1991) 2339.
[6] S. Takeno, J. Phys. Soc. Jpn. 58 (1989) 759.
[7] A.S. Davydov, Theory of Molecular Excitons, Plenum Press, New York, 1971.
[8] Y. Ishimori, Progr. Theor. Phys. 68 (1982) 402.
[9] P. Woafo, J.R. Kenne, T.C. Kofane, J. Phys.: Condens. Matter 5 (1993) L123.
[10] G.A. Baker Jr., Phys. Rev. 122 (1961) 1477; A.M. Kac, B.C. Helfand, J. Math. Phys. 4 (1972) 1078.
[11] L. Vazquez, W.A.B. Evans, G. Rickayzen, Phys. Lett. A 189 (1994) 454.
[12] Yu. Gaididei, N. Flytzanis, A. Neuper, F.G. Mertens, Phys. Rev. Lett. 75 (1995) 2240.
[13] O.M. Braun, Yu.S. Kivshar, I.I. Zelenskaya, Phys. Rev. B 41 (1990) 7118; A. Dikande, T.C. Kofane, Physica D 83 (1995) 450; G.L. Alfimov, V.M. Eleonskii, N.E. Kulagin, N.V. Mitskevich, Chaos 3 (1993) 405.
[14] Yu.B. Gaididei, S.F. Mingaleev, P.L. Christiansen, K.Ø. Rasmussen, Phys. Lett. A 222 (1996) 152.
[15] O. Bang, P.L. Christiansen, F. If, K.Ø. Rasmussen, Yu.B. Gaididei, Phys. Rev. E 49 (1994) 4627; P.L. Christiansen, Yu.B. Gaididei, M. Johansson, K.Ø. Rasmussen, I.I. Yakimenko, Phys. Rev. E 54 (1996) 924.
[16] Yu.B. Gaididei, S.F. Mingaleev, P.L. Christiansen, K.Ø. Rasmussen, Phys. Rev. E 55 (1997) 6141.
[17] P.L. Christiansen, Yu.B. Gaididei, K.Ø. Rasmussen, V.K. Mezentsev, J. Juul Rasmussen, Phys. Rev. B 54 (1996) 900.
[18] E.W. Laedke, K.H. Spatschek, S.K. Turitsyn, Phys. Rev. Lett. 73 (1994) 1055.
[19] L.D. Landau, E.M. Lifshitz, Statistical Physics, Pergamon Press, London, 1959
[20] D. Cai, A.R. Bishop, N. Grønbech-Jensen, Phys. Rev. Lett. 72 (1994) 591.
[21] M.L. Glasser, V.G. Papageorgiou, T.C. Bountis, SIAM J. Appl. Math. 49 (1989) 692.
[22] W. Magnus, F. Oberhettinger, R.P. Soni, Formulas and Theorems for the Special Functions of Mathematical Physics, Springer, Berlin, 1966.

[23] A.A. Vakhnenko, Yu.B. Gaididei, Teor. Mat. Fiz. 68 (1986) 350; Theor. Math. Phys. 68 (1987) 873.
[24] D. Cai, A.R. Bishop, N. Grønbech-Jensen, Phys. Rev. E 53 (1996) 4131.
[25] M.I. Molina, G.P. Tsironis, Physica D 65 (1993) 267; L.J. Bernstein, K.W. DeLong, N. Finlayson, Phys. Lett. A 181 (1993) 135; M. Johansson, M. Hörnquist, R. Riklund, Phys. Rev. B 52 (1995) 231.
[26] P.L. Christiansen, Yu.B. Gaididei, M. Johansson, K.Ø. Rasmussen, Phys. Rev. B 55 (1996) 5759.